Superlattice effect in the transport properties of Ni/Co multilayers

D. Lederman[a,1], J.M. Gallego[b,*], S. Kim[a], I.K. Schuller[a]

[a] *Physics Department 0319, University of California, San Diego, La Jolla, CA 92093-0319 USA*
[b] *Instituto de Ciencia de Materiales, Consejo Superior de Investigaciones Científicas, Cantoblanco, 28049 Madrid, Spain*

Abstract

The low-temperature transport properties of Ni/Co superlattices were systematically studied. While the resistivity, anisotropic magnetoresistance and anomalous Hall coefficient oscillate as functions of Co and/or Ni layer thicknesses, the ordinary Hall coefficient does not. These oscillations are interpreted as a true superlattice effect, since they disappear when the number of bilayer periods is decreased. © 1998 Elsevier Science B.V. All rights reserved.

1. Introduction

Since the discovery of the giant magnetoresistance (GMR) effect in Fe/Cr multilayers [1], the transport and magnetic properties of metallic multilayers, especially those with one magnetic component, have been the subject of many studies. In these systems, the coupling between the magnetic layers oscillates between ferromagnetic (F) and antiferromagnetic (AF) as a function of the nonmagnetic layer thickness [2]. It was recently shown that the coupling [3] and magnetoresistance [4] also oscillate as functions of the magnetic layer thickness in Fe/Cr and Co/Cu multilayers.

Although the exact mechanism responsible for these phenomena is not completely understood, the theoretical interpretations of the oscillatory coupling and the GMR effect are somewhat related. Both effects are thought to be due to the propagation of spin-polarized electrons across the nonmagnetic layers, with the spin-up and spin-down electrons having different reflection coefficients at the interfaces [5]. When the coupling between the magnetic layers is ferromagnetic, the spin-up electrons are weakly scattered in comparison with the spin-down electrons, which results in a low resistivity. In the AF configuration, electrons with different

---

* Corresponding author. Tel.: + 34 1 3349090; fax: + 34 1 3720623; e-mail: immgv84@pinar2.csic.es.

[1] Present address: Physics Department, West Virginia University, Morgantown, WV 26506-6315, USA.

spins are equally scattered and the resistivity is higher. Thus, GMR is observed when an external magnetic field is applied such that the AF configuration goes through a spin-flop transition, converting the AF configuration into the F configuration. The oscillatory behavior of the magnetic coupling produces oscillations in the magnetoresistance, being 'giant' when the coupling between the magnetic layers is AF in the zero-field configuration.

For this mechanism to be valid, the electrons' mean free path (MFP) must be of the order of the nonmagnetic layer thickness, in order for the electrons to be significantly affected by the relative orientation of adjacent magnetic layers. Within this framework, however, GMR is not a superlattice effect, in the sense that coupling or electronic transport across several superlattice periods is not required. In fact, the saturation resistivity in magnetic multilayers (or the zero-field resistivity in nonmagnetic multilayers), generally increases smoothly when decreasing the modulation wavelength, Λ, for *every system* reported to date [6–18]. In most systems, and in certain thickness ranges, $\rho \propto \Lambda^{-1}$, which implies that the MFPs in individual layers are limited by the layers' thicknesses [10]. A simple model consisting of electrically decoupled layers easily explains this increase [13]. Within this model, the electronic MFP is limited by the layer thickness, since the interface electron scattering is assumed to be entirely diffuse. Thus, the individual layers are treated as independent parallel resistors, with the resistivity of each single layer increasing as the thickness is decreased according to the classic Fuchs–Sondheimer theory [19] with $p = 0$, where p is the fraction of the electrons that is scattered elastically at the interfaces. Recent calculations show this ($p = 0$) to be the case for most systems [20].

Only a small number of true superlattice effects have been experimentally observed in metals. These include the appearance of superlattice Bragg peaks in X-ray diffraction [21], the collective behavior of magnons in magnetic/nonmagnetic superlattices [22] and the opening of superlattice gaps in the electronic band structure [23]. It was recently reported that in Ni/Co superlattices the resistivity displays an oscillatory behavior with the Ni and/or Co layer thicknesses [24]. This was shown to be a true superlattice effect, since the oscillations disappear when the number of bilayers is decreased. This constitutes the first experimental observation where the resistivity does not increase monotonically as the layer thickness is decreased [6–18].

In this paper, we report on a detailed study of the magnetotransport properties of Ni/Co superlattices, including Hall effect measurements. We show that, besides the resistivity, the anisotropic magnetoresistance and the extraordinary Hall coefficient have similar oscillatory behaviors. On the other hand, the ordinary Hall coefficient behaves as a weighted average of the bulk Ni and Co Hall coefficients. This means that the oscillations are not due to periodic variations in the *total* number of electrons enclosed by the Fermi surfaces, but to periodic variations in the density of states at the Fermi level and/or changes in the scattering matrix elements due to the superlattice structure.

2. Experimental and structural characterization

Ni/Co superlattices (denoted here as $(Ni_{dNi}Co_{dCo})_N$, where dNi and dCo are the thicknesses in Å of the Ni and Co layers, respectively, and N is the total number of periods), were grown on sapphire substrates $(Al_2O_3(1\ 1\ \bar{2}\ 0))$ by molecular beam epitaxy (MBE). The base pressure in the growth chamber was in the low 10^{-10} Torr range, and did not exceed 5×10^{-9} Torr during growth. Ni and Co were deposited using two independent electron guns with computer-controlled pneumatic shutters. The thickness of the deposited material was monitored by two calibrated electron impact emission spectroscopy sensors. The evaporation rates were fixed at ~ 0.1 Å/s for Ni and ~ 0.05 Å/s for Co. A ~ 50 Å Co buffer layer was deposited at $350°C$ on the sapphire substrate. The Ni/Co multilayers, approximately 1000 Å thick, were grown at $150°C$ on these buffer layers.

The multilayers structure was characterized in situ using high- and low-energy electron diffraction (RHEED and LEED) and Auger electron spectroscopy (AES), and ex situ with X-ray diffraction, using Cu K_α radiation ($\lambda \approx 1.5418$ Å) from a 12 kW rotating anode X-ray diffractometer. A detailed

report about the structural characterization can be found elsewhere [25]. Here we reproduce only the most relevant results.

Ni/Co multilayers grow epitaxially on sapphire, both Ni and Co in the FCC structure for all the layer thicknesses here reported, with NiCo(1 1 1)∥ Al$_2$O$_3$(1 1 $\bar{2}$ 0), and with a crystalline coherence length of ∼ 700–800 Å, i.e., almost equal to the whole superlattice thickness. The artificial periodicity was confirmed by AES and X-ray diffraction. Even for the thinner layers here reported, both high- and low-angle superlattice peaks were clearly visible. Also, from AES it was concluded that the Ni/Co interface is very sharp, the thickness of the interdiffused region having an upper limit of ∼2–3 monolayers (MLs). The multilayers are lattice matched in the plane of the film, i.e., both Ni and Co share the same in-plane lattice parameter. There are four different types of in-plain domains, each with a definite epitaxial relationship with the sapphire substrate. The in-plane domain size ranges between 100 and 200 Å. In summary, the Ni/Co multilayers reported here are *quasi*-single-crystalline, i.e., crystalline in the growth direction, but with twinned domains in the plane of the film [25].

The transport properties were measured using standard AC techniques on photolithographically patterned samples with a conventional four-lead geometry. Magnetoresistance and Hall effect were measured at room and low temperature ($T = 4.2$ K), with the current flowing in the plane of the film. In the first case, the resistivity was measured as a function of the applied magnetic field (up to 5 T), with the field both parallel and perpendicular to the current, but always in the plane of the superlattice. The Hall effect, as usual, was measured with the magnetic field perpendicular both to the current and the sample surface.

3. Resistivity measurements

In order to clarify the notation, Fig. 1a shows typical resistivity measurements as functions of the applied magnetic field (with the field both parallel and perpendicular to the current). Although the magnetoresistance can be as large as ∼15% for some of the grown samples, this is not the so-called
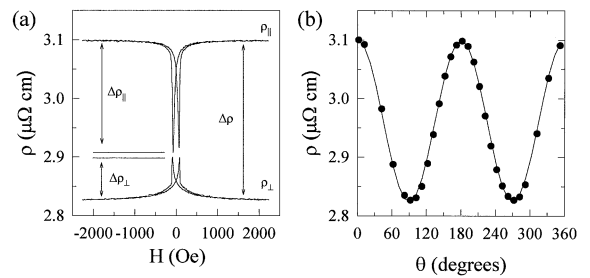
Fig. 1. (a) Resistivity as a function of the intensity of the magnetic field when applied parallel ($\rho_{\parallel}$) and perpendicular ($\rho_{\perp}$) to the current. (b) Saturation resistivity as a function of the angle between the current and the applied magnetic field for a (Ni$_{42}$Co$_{58}$)$_{10}$ superlattice. The solid line is a least-squares fit to Eq. (1).

GMR effect. As previously reported [26], the parallel magnetoresistance in Ni/Co superlattices is positive, i.e., the resistivity increases with the magnetic field, while the perpendicular magnetoresistance is negative. This is the so-called anisotropic magnetoresistance (AMR), common to almost all ferromagnetic materials [27]. In this sense, Ni/Co superlattices behave like ordinary ferromagnetic materials. In contrast, the GMR effect is always negative, regardless of the electrical current configuration, the resistivity being large in the AF configuration (zero field) and small when the sample is magnetically saturated (high field). In Ni/Co superlattices, the short-range exchange interaction dominates and no GMR is observed.

This can be proved by measuring the saturation resistivity, $\rho(\theta)$, as a function of the angle between the magnetic field and the current direction (Fig. 1b). For single-domain films where the magnetization M makes an angle θ with the current I, the AMR effect is usually described by [27]

$$\rho(\theta) = \rho_{\perp} + \Delta\rho \cos^2 \theta \qquad (1)$$

where $\rho_{\perp}$ is the resistivity when the magnetic field is applied perpendicular to the current, extrapolated to zero field, and $\Delta\rho = \rho_{\parallel} - \rho_{\perp}$ is the anisotropic magnetoresistivity, with $\rho_{\parallel}$ being the resistivity when the magnetic field is parallel to the current, also extrapolated to zero field. (In our case, since the resistivity in both configurations saturates for moderate magnetic fields, $\rho_{\parallel}$ and $\rho_{\perp}$ can be set equal to the respective saturation resistivities with

negligible error.) The solid line is a least-squares fit of the experimental data to Eq. (1). The good quality of the fit shows that, in this system, any change in resistivity with magnetic field is entirely due to the AMR effect.

The resistivity of the zero-field state in magnetic materials depends on the exact domain configuration. So it is history dependent and not a well-defined quantity. For bulk materials, an average resistivity is usually defined as $\rho_0 = (\rho_\parallel + 2\rho_\perp)/3$. For thin films, where the magnetization usually lies in the plane of the film (as is the case for these superlattices), the expression $\rho_0 = (\rho_\parallel + \rho_\perp)/2$ seems more appropriate, since only one direction of the magnetization perpendicular to the current is allowed. However, the use of either definition does not alter the results of this paper, since the changes in resistivity described below are in all cases much greater than $\Delta\rho$. The anisotropic magnetoresistivity ratio is defined as $\Delta\rho/\rho_0$.

Although the changes in resistivity with applied field below saturation, $\Delta\rho_\parallel$ and $\Delta\rho_\perp$, depend on the detailed magnetic domains configuration and magnetization processes in the superlattice, this is not true for $\Delta\rho$ since it is calculated from resistivities of two configurations where the sample is magnetically saturated.

Fig. 2a and Fig. 2b show ρ_0 and $\Delta\rho$, as functions of Λ, for a series of Ni/Co superlattices with composition $(Ni_{0.4\Lambda}Co_{0.6\Lambda})_N$, i.e., with the same relative concentration of Ni and Co (dNi/dCo $= \frac{2}{3}$), but different modulation wavelengths. It is clear from the results that both ρ_0 and $\Delta\rho$ are not monotonous functions of Λ, but display a series of maxima and minima, whose positions is approximately the same for both quantities. The period of these oscillations, for the first two maxima, is ~ 20 Å. As stated above, this oscillatory behavior is different from that found in other metallic multilayers, where the resistivity always increases smoothly when Λ decreases [6–18].

Figs. 3 and 4 (panels (a) and (b)) show ρ_0 and $\Delta\rho$ for two other series of samples as functions of the Co and Ni layer thicknesses. In the first series (Fig. 3), the Ni layer thickness was kept constant at dNi = 42 Å while dCo was varied between 5 and 130 Å. For the second series (Fig. 4), dCo = 18 Å, while dNi was swept between 4 and 45 Å. Also in
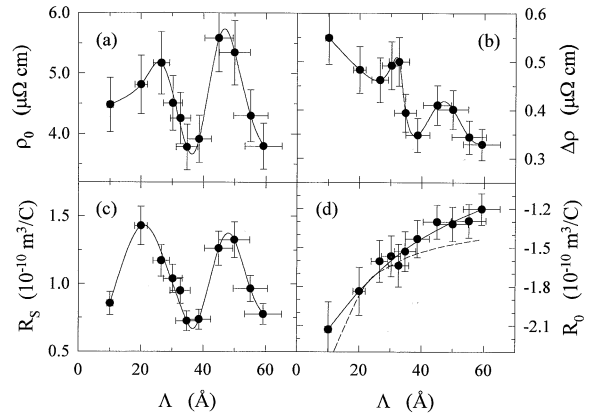
Fig. 2. Resistivity, ρ_0, magnetoresistivity, $\Delta\rho$, extraordinary Hall coefficient, R_S, and ordinary Hall coefficient, R_0, for a series of Ni/Co superlattices with dCo/dNi $= \frac{3}{2}$ as a function of Λ. The solid lines are guides to the eye. The dashed line in (d) is a calculation using Eq. (4).
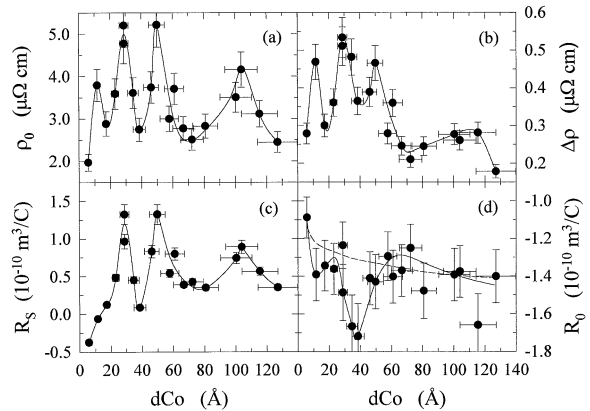
Fig. 3. Resistivity, ρ_0, magnetoresistivity, $\Delta\rho$, extraordinary Hall coefficient, R_S, and ordinary Hall coefficient, R_0, for a series of Ni/Co superlattices with dNi = 42 Å as a function of dCo [24]. The solid lines are guides to the eye. The dashed line in (d) is a calculation using Eq. (4).

these cases both quantities oscillate as functions of the Co and Ni layer thicknesses, with approximately the same period (~ 20 Å). On the other hand, a series of samples with dCo = 6 Å (Fig. 5) only shows a sharp maximum when dNi ≈ 10 Å, with a small feature around dNi ≈ 32 Å perhaps present.

In every case, the amplitude of the oscillations (almost 100%) is well outside the measurement
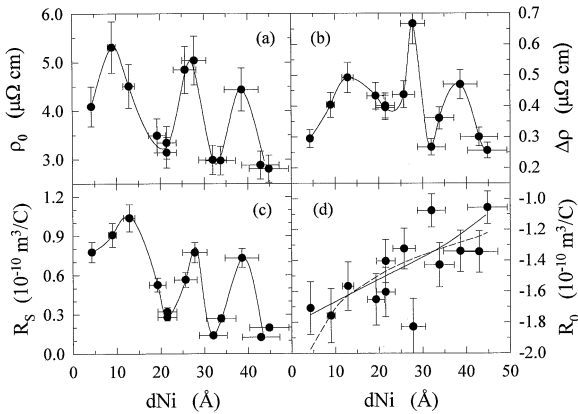
Fig. 4. Resistivity, ρ_0, magnetoresistivity, $\Delta\rho$, extraordinary Hall coefficient, R_S, and ordinary Hall coefficient, R_0, for a series of Ni/Co superlattices with $dCo = 18$ Å as a function of dNi [24]. The solid lines are guides to the eye. The dashed line in (d) is a calculation using Eq. (4).
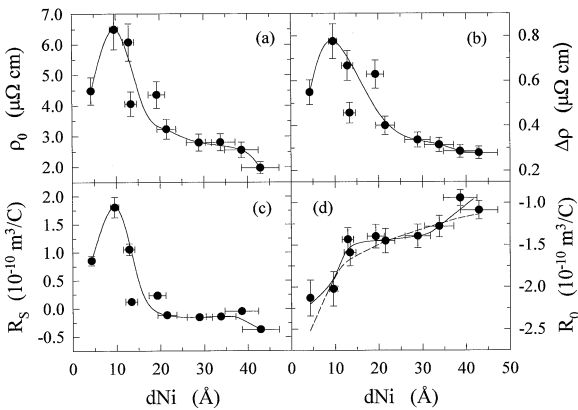
Fig. 5. Resistivity, ρ_0, magnetoresistivity, $\Delta\rho$, extraordinary Hall coefficient, R_S, and ordinary Hall coefficient, R_0, for a series of Ni/Co superlattices with $dCo = 6$ Å as a function of dNi. The solid lines are guides to the eye. The dashed line in (d) is a calculation using Eq. (4).

error, mainly due to thickness calibration uncertainty which is estimated to be $\sim 10\%$. Note that when two nominally identical samples were grown in two separate experimental runs, the values of ρ_0 and $\Delta\rho$ were reproduced to within 10%. The structure of the superlattices was thoroughly characterized [25], and no correlation was found between any structural parameter and the variations
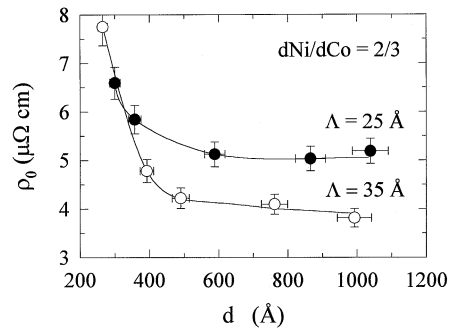
Fig. 6. Resistivity of two selected samples of the series with $dCo/dNi = \frac{3}{2}$ as a function of the total thickness d.

in the resistivity. Thus, these oscillations cannot be assigned to any kind of structural or disorder parameter variation with the layer thicknesses, and so must be of electronic origin.

The fact that the oscillatory behavior is a *true* superlattice effect was proven in Ref. [24], where it was clearly shown that the oscillations disappear as the number of bilayers in the superlattice decreases. Additional proof can be found in Fig. 6, which shows the resistivity, as a function of the *total* thickness d, varying N, of two other series of samples (one at the first maximum and the other at the first minimum in Fig. 2a). For large d ($N \sim 30$), the resistivity of the series with $\lambda = 25$ Å is greater than the resistivity of the series with $\lambda = 35$ Å, but when d (or N) decreases, the difference decreases, and when $d \approx 300$ Å, they tend to converge to the same value, which seems to demonstrate that at least ~ 8–10 periods are required to see the oscillatory effect.

A simple inspection of panels (a) and (c) of Figs. 2–5 indicates that ρ_0 and $\Delta\rho$ are closely related, although a simple linear relation is not enough to describe the experimental data, since $\Delta\rho/\rho_0$ depends on the Ni and Co individual layer thickenes and of the number of periods of the superlattice. It is clear from Fig. 7, however, that the AMR effect in Ni/Co superlattices is different from the one observed in the corresponding alloys. The solid line in this figure represents data measured at 20 K in bulk NiCo alloys [28]. Although $\Delta\rho/\rho_0$ shows a slight trend to decrease while increasing the Co content, when the Co percentage is
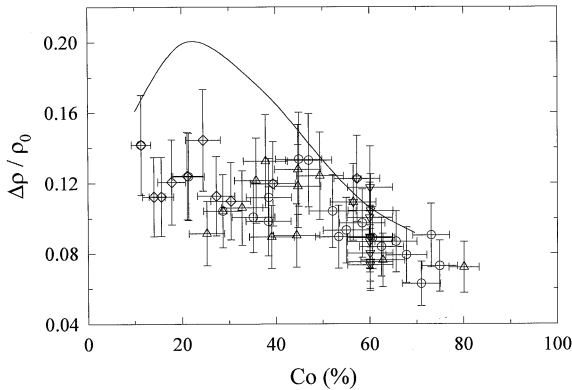
Fig. 7. Relationship between $\Delta\rho/\rho_0$ and the relative Co concentration for all the samples. ($\triangledown$) represents the data from Fig. 2, ($\bigcirc$) the data from Fig. 3, ($\triangle$) represents the data from Fig. 4, and ($\diamondsuit$) represents the data from Fig. 5. The solid line represents the data measured in bulk Ni/Co alloys.

below 50%, $\Delta\rho/\rho_0$ for the superlattices falls well below the data for bulk alloys, and does not clearly show the maximum at 20–30% Co present in these.

4. Hall effect measurements

To gain further insight into this new phenomenon, Hall effect measurements were carried out on the same set of samples. A typical Hall resistivity (ρ_{xy}) measurement as a function of the external magnetic field H, is shown in Fig. 8 for a $(Ni_{32}/Co_{18})_{20}$ superlattice. As in ordinary ferromagnets, ρ_{xy} has two contributions. One is the ordinary Hall effect due to the Lorentz force of the magnetic field on the conduction electrons, which is proportional to H, and is clearly present in ρ_{xy} as a linear contribution above saturation. The extrapolation to zero field of this line, however, does not go through the origin. This is due to the second contribution, the extraordinary Hall effect, present in all ferromagnetic materials [29]. A least-squares fit of the linear part, to the relation

$$\rho_H = R_0 H + 4\pi R_S M_S, \qquad (2)$$

where M_S is the saturation magnetization, gives the ordinary (R_0) and extraordinary (R_S) Hall coefficients. M_S was measured with a SQUID magnetometer at 10 K and, within the experimental error,
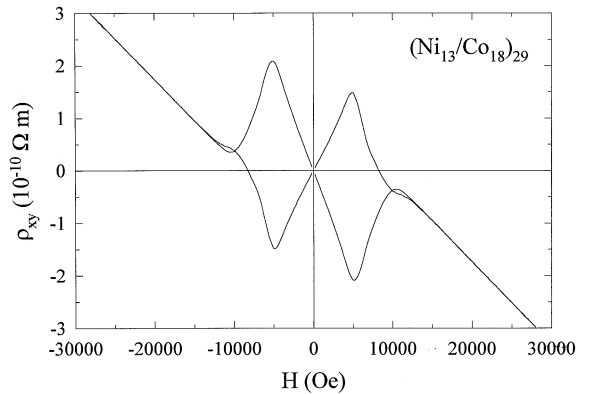
Fig. 8. Hall resistivity, ρ_{xy}, as a function of the magnetic field H for a $(Ni_{13}Co_{18})_{29}$ superlattice.

the measured values were consistent with the bulk values for Ni and Co.

The bottom panels in Figs. 2–5 show the results for R_0 and R_S for the four different series. Clearly, R_S exhibits the same oscillatory behavior as ρ_0 and $\Delta\rho$, with the same positions for the maxima and minima. (It has been recently reported that the extraordinary Hall effect also oscillates as a function of the Cu layer thickness in $Co_{90}Fe_{10}/Cu$ multilayers [30].) In contrast, R_0 behaves differently. The general trend of R_0 in the different series can be described by a weighted contribution of the interfaces and the Co and Ni layers with the equation

$$R_0 = \frac{(dNi - dint)R_{Ni} + (dCo - dint)R_{Co} + 2dint R_{NiCo}}{dNi + dCo}, \qquad (3)$$

where R_{Ni} and R_{Co} are the ordinary Hall coefficients for the Ni and Co layers, respectively, R_{NiCo} is the Hall coefficient of a Ni/Co alloy $dint$ thick formed at the interfaces. The fitting procedure yields $R_{Ni} = -0.8 \times 10^{-10}$ m³/C, $R_{Co} = -1.5 \times 10^{-10}$ m³/C, $R_{NiCo} = -2.2 \times 10^{-10}$ m³/C and $dint = 3$ Å, and the results are indicated in Figs. 2–5 with a dashed line. The values for R_{Ni} and R_{Co} are very close to the values measured in bulk Ni and Co [31], while R_{NiCo} is similar to the value measured in $Ni_{0.5}Co_{0.5}$ alloys [31]. The value
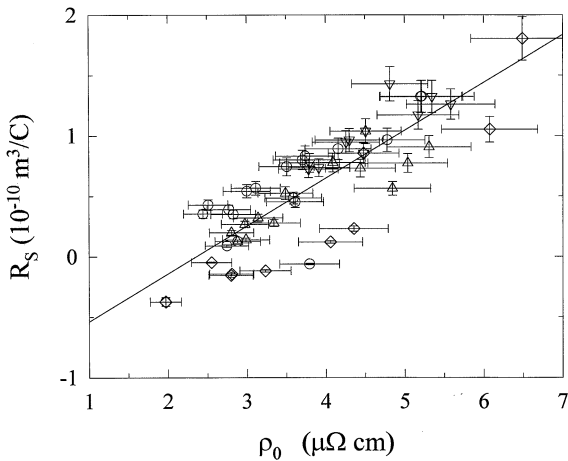
Fig. 9. The extraordinary Hall effect R_S versus ρ_0 for all the grown samples. Symbols as in Fig. 7. The solid line is the result of a least-squares fit to the data.

obtained for the thickness of this interface ($2d_{int} \approx 6$ Å), agrees with the results of the AES measurements taken during growth, which gave an upper limit of 4–6 Å for this thickness [25]. Thus, as Eq. (3) implies, the ordinary Hall coefficient of these Ni/Co superlattices looks just like a weighted average of the Hall coefficients of the Ni and Co layers and the NiCo alloy present at the interface.

On the other hand, as Fig. 9 shows, the R_S measurements correlate with ρ, which is the quantity that oscillates. From this figure, however, it is impossible to determine whether the dominant mechanism is the skew ($\propto \rho_0$) or side-jump ($\propto \rho_0^2$) scattering [32]. However, the fact that for some samples the R_S changes sign, is an indication that the dependence on ρ_0 is related to changes in the band structure of the sample with different Co and Ni periodicities. This is because both mechanisms depend on the spin–orbit coupling parameter, whose sign and magnitude depends on the position of the Fermi level with respect to the center of the d-electron band (see below) [32].

5. Discussion

The transport properties in transition metals and alloys can be described using Mott's two-current model [33]. Within this model, current is carried mostly by the 4s electrons. On the other hand, because the density of states at the Fermi level of the d electrons, $D_d(E_F)$, is large, the s–d interband transitions determine the resistivity in the paramagnetic state. Assuming that the spin direction does not change during these transitions, the current can be divided into two independent parts, one composed of the s↑ electrons (with resistivity $\rho_\uparrow$), and the other of the s↓ electrons (with resistivity $\rho_\downarrow$). Below the Curie temperature, and in the absence of spin–orbit coupling, the d↑ states are almost completely occupied. So the s↑ electrons can scatter only to other s↑ states. Hence, their resistivity is much smaller than for the s↓ electrons given the presence of empty d↓ states. Therefore, at low temperatures, the resistivity is determined mainly by the s↑–s↑ transitions, implying that $\rho_\downarrow > \rho_\uparrow$. In summary

$$\rho_0 = \frac{\rho_\uparrow \rho_\downarrow}{\rho_\uparrow + \rho_\downarrow}, \tag{4}$$

where, within the first Born approximation, and assuming $\rho_{ss\downarrow} \ll \rho_{sd\downarrow}$ [34]

$$\rho_\downarrow = \rho_{ss\downarrow} + \rho_{sd\downarrow} \approx \rho_{sd\downarrow}$$
$$= \frac{2\pi}{\hbar} \overline{|\langle \psi_k^s | \Delta V | \psi_{k'n'}^{d\downarrow} \rangle|^2} D_\downarrow^d(E_F) \frac{m_s}{n_s e^2}, \tag{5}$$

$$\rho_\uparrow = \rho_{ss\uparrow} + \rho_{sd\uparrow}$$
$$= \frac{2\pi}{\hbar} \left(\overline{(1 - \cos\theta)|\langle \psi_k^s | \Delta V | \psi_{k'}^s \rangle|^2} D_\uparrow^s(E_F) \right.$$
$$\left. + \overline{|\langle \psi_k^s | \Delta V | \psi_{k'n'}^{d\uparrow} \rangle|^2} D_\uparrow^d(E_F) \right) \frac{m_s}{n_s e^2}. \tag{6}$$

$D_\uparrow^d$, $D_\uparrow^d$ and $D_\uparrow^s$ are the 3d and 4s densities of states for spin-up and spin-down bands, ΔV is the scattering potential, ψ_k^s, $\psi_{kn}^{d\uparrow}$ and $\psi_{kn}^{d\downarrow}$ are Bloch waves for the s band and the spin-up and spin-down d bands, m_s is the 4s electron effective mass, n_s is the 4s electron density, and θ is the angle between $\boldsymbol{k}$ and $\boldsymbol{k}'$. The horizontal bar indicates an average over the Fermi surface and over n'.

Variations in ρ_0 may result from changes in the matrix elements, $D_\downarrow^d(E_F)$, $D_\uparrow^d(E_F)$, $D_\uparrow^s(E_F)$, or n_s. As a first approach, we assume the matrix elements to be constant, as is often done for alloys (see below).

Since the oscillations in ρ_0 are not accompanied by oscillations in the ordinary Hall effect, changes in n_s cannot be responsible for the oscillatory behavior. Rather, the oscillations must originate from periodic changes in the density of states at the Fermi level due to the superlattice structure. Because the d↑ states are occupied at low temperatures (i.e., $D_\uparrow^d(E_F) \sim 0$), the oscillations must result from periodic variations in $D_\downarrow^d(E_F)$ or $D_\uparrow^s(E_F)$.

It is reasonable to assume that the most important band structure modifications due to the superlattice structure will take place along the growth direction, which for these Ni/Co superlattices is the FCC [1 1 1] direction. The band structure for Ni [35] and FCC Co [36] in the [1 1 1] direction are displayed in Fig. 10. In Ni, the $\Lambda_{3\downarrow}$ band (the top band in Fig. 10), which has a pronounced d character, is the only one that crosses the Fermi level (just at the edge of the zone) in this direction. In contrast, the Co band is displaced ~ 1 eV to higher energies, even though the dispersion is otherwise similar, and is always above the Fermi level. Assuming that the band structure of the superlattice is, to a first approximation, very similar to a weighted average of the band structures of its constituents [37], it seems very reasonable to assume that the $\Lambda_{3\downarrow}$ band of the superlattice will also cross (and will be the only one) the Fermi level in the [1 1 1] direction. As a consequence, we tentatively conclude that the oscillatory behavior of the resistivity must be due to periodic variations in $D_\downarrow^d(E_F)$.

The AMR effect has been thoroughly studied in 3d metals and alloys [27,38–40]. The most widely accepted explanation is based on Smit's original work [38]. Above, we assumed that at low temperatures the d↑ states are almost completely occupied. This is strictly true only in the absence of spin–orbit coupling. When this coupling is taken into account, there is some mixing of ↑ and ↓ states. In particular, even at $T = 0$, there will be some unoccupied d↑ states at the Fermi surface, which result in scattering of s↑ electrons into d↑ states. However, this mixing is not isotropic, because the magnetization direction provides an axis for the spin–orbit perturbation. It can be shown [38] that there will be a deficiency of hole–orbits perpendicular to the magnetization. The s electrons, when moving along the magnetization direction, are
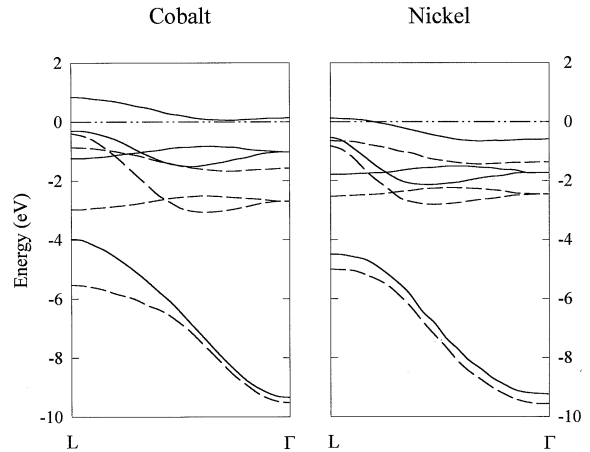
Fig. 10. Calculated band structures for FCC Co [36] and Ni [35].

more easily trapped than in the transverse direction, and since the resistance is mainly determined by the scattering of the electrons moving in the direction of the current, $\rho_\parallel > \rho_\perp$. Then, periodic variations in the density of states at the Fermi level of the d↓ states produce periodic variations in the amount of mixing. In this way, $\Delta\rho \propto \rho_0$, because the oscillations of $\Delta\rho$ and ρ_0 originate from the same mechanism, namely, periodic variations in $D_\downarrow^d(E_F)$.

Similar considerations can explain the oscillations in the extraordinary Hall coefficient, R_S. Although the theoretical treatment is much more complicated [29,32,40,41], the extraordinary Hall effect is thought to result from the asymmetric scattering of conduction electrons. Although there are several mechanisms that could give rise to this scattering [29], all of them are proportional to a spin–orbit coupling. Neglecting the exact nature of the scattering mechanism, the magnitude of the effect will depend on the number of scattering processes, which is proportional to the density of states at the Fermi level. In fact, according to most theories [32,42], the properties of the 3d states lying at the Fermi level determine the value of R_S. Thus, it is natural that ρ_0 and R_S should be correlated.

The problem is, therefore, identifying the mechanism responsible for the periodic variations in the density of states at the Fermi level as the layer

thicknesses are changed. In this sense, it is important to point out the low values of the measured resistivities, which are only slightly higher than the corresponding values in bulk Ni/Co alloys, and, to our knowledge, are the lowest values ever reported for any type of metallic superlattice with similar layers thicknesses (they are, e.g., between 3 and 4 times lower than the resistivities measured in Co/Cu multilayers [16], which is somewhat surprising, since the resistivity of Cu is ~ 4 times lower than the resistivity of Ni). This seems to be an indication of a longer electron MFP in the Ni/Co superlattices, probably due to a larger structural coherence length. The MFP calculated using the Sommerfeld approximation [43] ranges between 100 and 200 Å, which is larger than the multilayer modulation wavelength, indicating that the interface scattering is weak. (In fact, the MFP seems to be limited by the *in-plane* grain size, which ranges between 100 and 200 Å [25].) Since the vertical structural coherence length is ~ 700–800 Å, extended electronic states may exist throughout *the entire superlattice thickness*. These new Bloch states will be sensitive to the superlattice periodicity, thus modifying the electronic band structure.

The new band structure of the superlattice may give rise to periodic variations in the density of states at the Fermi level in different ways. One mechanism is the crossing of quantum wells states with the Fermi level as the layer thickness changes [44]. Since there is an energy window of ~ 0.6 eV where the (1 1 1) projections of the $\Lambda_{3\downarrow}$ bands of Ni and Co do not overlap (Fig. 10), quantum well states in the Co layers could be expected. When the thickness of the Co layers increases, these states move up in energy, periodically crossing the Fermi level and producing oscillations in $D(E_F)$. However, this is *not* a superlattice effect, since quantum wells can exist in single layers, and therefore cannot explain the disappearance of the oscillations when the number of periods is reduced (Fig. 6). Two other closely related explanations have been recently proposed. The first one [45] relies on the existence of *localized* states, created by disorder at the Ni/Co interfaces, that periodically cross the Fermi level as the layers thicknesses change. The second one [46] proposes that the resistivity oscillations are due to the resonant scattering of the majority spin-up s-electrons against the mainly d-character quantum well states induced in the Ni layers.

A true superlattice effect results from the opening of mini-gaps at the band edges [37]. When the modulation wavelength Λ is such that the Fermi level crosses an electronic band just at the edge of the *superlattice* Brillouin zone, where an energy gap exists, the density of states at the Fermi level decreases. This decrease will be almost periodic, since doubling Λ will again cause the electronic band to cross the Fermi level at the edge of the new superlattice Brillouin zone. The difficulty with this explanation is that the superlattice periodicity exists only along the growth direction, while the transport measurements reported here were performed with the current in the plane of the film.

A more plausible explanation is probably a combination of these models. Recent realistic band structure calculations for Co/Cu(1 0 0) superlattices [47] have proven the existence of flat bands, almost dispersionless in an extended k-space region, in the *in-plane* direction, as a consequence of an enhancement of the effective mass of the superlattice states. The energies of these bands change depending on the layer thicknesses, and periodically cross the Fermi level. Actually, the spatially averaged *total* DOS at the Fermi level oscillates as a function of the Co layer thickness [47]. The only requirement for the development of a flat band at the superlattice Fermi surface is the existence of a narrow band close to E_F in the superlattice constituents, a requirement which is fullfilled for both Co and Ni (Fig. 10). Although the amplitude of these oscillations in Co/Cu ($\sim 10\%$) seems rather small, the results are not directly comparable with the experimental results presented here. Besides, the role of the different states (of s–p or d character) in the transport properties needs to be taken into account.

Regardless of the exact mechanism, the oscillatory behavior in the transport properties in Ni/Co superlattices seems to be due to periodic variation in the density of states at the Fermi level of the d↓ electrons when the layer thicknesses changes. This may give raise to resistivity changes either directly or through resonant s–d scattering. Detailed and realistic band structure calculations for Ni/Co

(1 1 1) superlattices may be useful in determining the correct explanation.

6. Conclusions

In summary, oscillations in the transport properties (resistivity, anisotropic magnetoresistance and extraordinary Hall coefficient) as functions of the layer thicknesses were observed in Ni/Co multilayers. This oscillatory behavior was shown to be a superlattice effect, since the oscillations disappear when the number of periods in the superlattice is decreased. Since the ordinary Hall coefficient does not oscillate, the oscillatory behavior is produced by periodic changes in the density of states at the Fermi level due to the superlattice structure.

The discovery of superlattice effects in metallic multilayers has important consequences for transport theories of layered systems, which are currently based primarily on the Boltzmann equation and almost totally disregard the detailed band structure of the superlattice [48]. A complete explanation of the phenomena described in this paper must rely on calculations which take into account the superlattice periodicity.

Acknowledgements

References

[1] M.N. Baibich, J.M. Broto, A. Fert, F. Nguyen van Dau, F. Petroff, P.E. Etienne, G. Creuzet, A. Friedrich, J. Chazelas, Phys. Rev. Lett. 61 (1988) 2472.

[2] S.S.P. Parkin, Phys. Rev. Lett. 64 (1990) 2304.

[3] P.J.H. Bloemen, M.T. Johnson, M.T.H. van de Vorst, R. Coehoorn, J.J. de Vries, R. Jungblut, J. aan de Stegge, A. Reinders, W.J.M. de Jonge, Phys. Rev. Lett. 72 (1994) 764.

[4] S.N. Okuno, K. Inomata, Phys. Rev. Lett. 72 (1994) 1553.

[5] A. Fert, P. Grünberg, A. Barthélemy, F. Petroff, W. Zinn, J. Magn. Magn. Mater. 140–144 (1995) 1.

[6] I.K. Schuller, C.M. Falco, in: Inhomogeneous Superconductors-1979, AIP Conf. Proc., vol. 58, 1979, p. 197.

[7] T.R. Werner, I. Banerjee, Q.S. Yang, C.M. Falco, I.K. Schuller, Phys. Rev. B 26 (1982) 2224.

[8] P.F. Carcia, A. Suna, J. Appl. Phys. 54 (1983) 2000.

[9] M.R. Khan, C.S.L. Chun, G.P. Felcher, M. Grimsditch, A. Kueny, C.M. Falco, I.K. Schuller, Phys. Rev. B 27 (1983) 7186.

[10] M. Gurvitch, Phys. Rev. B 34 (1986) 540.

[11] T. Kaneko, T. Sasaki, M. Sakuda, R. Yamamoto, T. Nakamura, H. Yamamoto, S. Tanaka, J. Phys. F 18 (1988) 2053.

[12] J.W.C. de Vries, F.J.A. den Broeder, J. Phys. F 18 (1988) 2635.

[13] G. Reiss, K. Kapfberger, G. Meier, J. Vancea, H. Hoffmann, J. Phys.: Condens. Matter 1 (1989) 1275.

[14] H. Sato, I. Sakamoto, C. Fierz, J. Phys.: Condens. Matter 3 (1991) 9067.

[15] W.H. Sae, T. Kaizuka, R. Yamamoto, T. Mitsuhashi, J. Magn. Magn. Mater. 126 (1993) 457.

[16] J.L. Duvail, A. Fert, L.G. Pereira, D.K. Lottis, J. Appl. Phys. 75 (1994) 7070.

[17] H. Sato, T. Matsudai, W. Abdul-Razzaq, C. Fierz, P.A. Schroeder, J. Phys.: Condens. Matter 6 (1994) 6151.

[18] Y. Kobayashi, H. Sato, Y. Aoki, A. Kamijo, J. Phys.: Condens. Matter 6 (1994) 7255.

[19] E.H. Sondheimer, Adv. Phys. 1 (1952) 1.

[20] Y. Inoue, K. Mae, N. Kyuno, T. Kaneko, R. Yamamoto, J. Magn. Magn. Mater. 126 (1993) 475.

[21] I.K. Schuller, Phys. Rev. Lett. 44 (1980) 1597.

[22] M. Grimsditch, M.R. Khan, A. Kueny, I.K. Schuller, Phys. Rev. Lett. 51 (1983) 498.

[23] T. Miller, T.C. Chiang, Phys. Rev. Lett. 68 (1992) 3339.

[24] J.M. Gallego, D. Lederman, S. Kim, I.K. Schuller, Phys. Rev. Lett. 74 (1995) 4515.

[25] J.M. Gallego, S. Kim, T.J. Moran, D. Lederman, I.K. Schuller, Phys. Rev. B 51 (1995) 2550.

[26] J.M. Gallego, D. Lederman, T.J. Moran, I.K. Schuller, Appl. Phys. Lett. 64 (1994) 2590.

[27] T.R. McGuire, R.I. Potter, IEEE Trans. Magn. 11 (1975) 1018.

[28] H.C. Van Elst, Physica 25 (1959) 708.

[29] C.M. Hurd, The Hall Effect in Metals and Alloys, Plenum Press, New York, 1972.

[30] H. Sato, Y. Kobayashi, Y. Aoki, Y. Saito, K. Inomata, Phys. Rev. B 52 (1995) R9823.

[31] S. Foner, E.M. Pugh, Phys. Rev. 91 (1953) 20.

[32] L. Berger, G. Bergmann, in: C.L. Chien, C.R Westgate (Eds.), The Hall Effect and Its Applications, Plenum Press, New York, 1979, p. 55.

[33] N.F. Mott, Proc. Roy. Soc. London A 153 (1936) 699.

[34] L. Berger, J. Appl. Phys. 67 (1990) 5549.

[35] D.A. Papaconstantopoulos, Handbook of the Band Structure of Elemental Solids, Plenum Press, New York, 1986.

[36] J.L. Pérez-Díaz, M.C. Muñoz, Phys. Rev. B 50 (1994) 8824.

[37] T.C. Chiang, T. Miller, W.E. McMahon, Phys. Rev. B 50 (1994) 11102. This is probably a good approximation for s–p bands. However, its validity is not clear for a complicated narrow band.

[38] J. Smit, Physica 16 (1951) 612.

[39] I.A. Campbell, A. Fert, O. Jaoul, J. Phys. C 3 (1970) S95.

[40] I.A. Campbell, A. Fert, in: E.P. Wohlfarth (Ed.), Ferromagnetic Materials, vol. 3, ch. 9, North-Holland, Amsterdam, 1982.

[41] J. Smit, Physica 24 (1958) 39.

[42] L. Berger, Physica 30 (1964) 1141.

[43] N.W. Ashcroft, N.D. Mermin, Solid State Physics, Saunders College, Philadelphia, 1976, p. 52.

[44] J.E. Ortega, F.J. Himpsel, Phys. Rev. Lett. 69 (1992) 844.

[45] S. Kim, D. Lederman, J.M. Gallego, I.K. Schuller, Phys. Rev. B 54 (1996) R5291.

[46] M. Kiwi, A.M. Llois, R. Ramírez, M. Weissmann, unpublished.

[47] J.L. Pérez-Díaz, M.C. Muñoz, Phys. Rev. Lett. 76 (1996) 4967.

[48] X.G. Zhang, W.H. Butler, Phys. Rev. B 51 (1995) 10085.